

# Weakly-Supervised Semantic Segmentation of Ships Using Thermal Imagery

Rushil Joshi<sup>\*†</sup>, Ethan Adams<sup>\*‡</sup>, Matthew Ziemann<sup>§†</sup> and Christopher A. Metzler<sup>†</sup>

<sup>†</sup> University of Maryland, College Park, <sup>‡</sup> University of North Texas, <sup>§</sup> DEVCOM Army Research Laboratory

\* Equal Contributions

Email: rjoshi23@umd.edu, metzler@umd.edu

**Abstract**—The United States coastline spans 95,471 miles [1]; a distance that cannot be effectively patrolled or secured by manual human effort alone. Unmanned Aerial Vehicles (UAVs) equipped with infrared cameras and deep-learning based algorithms represent a more efficient alternative for identifying and segmenting objects of interest—namely, ships. However, standard approaches to training these algorithms require large-scale datasets of densely labeled infrared maritime images. Such datasets are not publicly available and manually annotating every pixel in a large-scale dataset would have an extreme labor cost.

In this work we demonstrate that, in the context of segmenting ships in infrared imagery, weakly-supervising an algorithm with sparsely labeled data can drastically reduce data labeling costs with minimal impact on system performance. We apply weakly-supervised learning to an unlabeled dataset of 7055 infrared images sourced from the Naval Air Warfare Center Aircraft Division (NAWCAD). We find that by sparsely labeling only 32 points per image, weakly-supervised segmentation models can still effectively detect and segment ships, with a Jaccard score of up to 0.756.

## I. INTRODUCTION

Deep object detection models have demonstrated the ability to find and classify objects of interest - an essential asset to the interest of national security [2]. Due to the breadth of the United States coastline, ships and other watercraft are among the highest-priority objects of interest. Automating the task through the application of object detection networks allows for efficient, yet accurate detection at comparable-to-human accuracy.

Neural networks represent the state-of-the-art solution for identifying objects of interest for UAV operators in the thermal domain, which is commonly used in maritime environments. Deep convolutional neural networks are able to detect objects of interest and segment image into individual classes with high accuracy in the visual spectrum, as well as the infrared spectrum [3][4]. Image segmentation offers greater detail than detection within each prediction, since each pixel has an associated predicted class. In addition to visible spectrum images, neural-based segmentation has shown quality results for thermal images [5, 6] as well.

Traditionally, segmentation methods require ground truth annotations in the form of masks, marking each pixel in the image with an object classification. However, this approach requires an extensive amount of time and human resources. An example of a full segmentation mask is displayed in Figure 1. The introduction of weakly-supervised learning [7, 8, 9, 10],

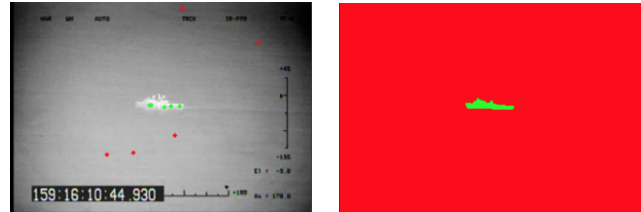


Fig. 1: Sparse annotations (left) versus dense annotations (right). Sparse annotations are far easier to generate.

allows for annotators to quickly and efficiently perform sparse annotation rather than annotating fully-segmented mask, without compromising on segmentation performance. The success of image segmentation trained on weakly-supervised annotations dispels standard of requiring fully-segmented mask annotations.

This paper expands on the usefulness of the proposed methods — namely, point-wise and squiggle-wise annotation — to annotate and train a model for segmentation using weakly-labeled infrared images. By utilizing a modified U-Net segmentation architecture and point supervision on thermal images, we illustrate the effectivity of using point-wise annotations to utilize object segmentation with minimal truth labels, and therefore minimal annotation work. We also demonstrate that this method is robust to constraints presented in our study, including but not limited to poor image quality, noise due to varying environmental conditions, a minimal number of annotations, and limited training times.

## II. RELATED WORK

### A. Infrared Domain Image Segmentation

Image segmentation is among the most popular and widely-researched computer vision problems, across a wide variety of imaging domains, including the visible spectrum (RGB) and infrared (IR) domains. State-of-the-art neural-based image segmentation solutions generally make use of an encoder-decoder architecture, often with additional feature fusion modifications such as skip connections and residuals. In the encoder, input images are reduced to a low-resolution feature space, with generalized features learned earlier and image-specific features learned further into the network. The decoder learns to up-sample latent features learned by the encoder and project them back into a segmentation mask, for which

each pixel is assigned a class probability. To preserve spatial information within the network, architectures such as U-Net [11] and SegNet [12] utilize skip connections, concatenating previously-learned features to latter layer inputs. Other state-of-the-art segmentation networks, such as Mask R-CNN [13], use a pre-trained backbone convolutional neural network in tandem with a region proposal network to learn latent feature mappings, which are then used to generate a segmentation mask.

Specifically for images in the IR domain, skip-enabled encoder-decoder architectures have a history of success for various segmentation tasks. [14] uses a modified U-Net architecture with residual learning capability for the task of segmenting photovoltaic panels within thermal images, scoring a Jaccard index score of 92.65% with a standard U-Net and over 94% using the modified architecture. Furthermore, [5] provides a comprehensive comparative analysis across various thermal segmentation datasets, along with performance metrics from U-Net and other similar segmentation architectures (SegNet, MFNet).

While state-of-the-art approaches generally perform well on most image segmentation datasets, even with a limited number of samples, annotation of segmentation masks is significantly more costly when considering the time required to annotate a single image. Large, generalizable segmentation datasets that are fully and accurately painted with labels, such as MSCOCO [15], demonstrably allow a network to learn large-scale features that can be used to pre-train for a smaller, more specific task, as shown in [7]. However, annotating for a custom segmentation task can take exponentially longer amounts of time as the number of classes and complexity of the images increases.

### B. Weakly-Supervised Segmentation

Due to the significant increase in cost of full segmentation mask annotation compared to other vision-based tasks, existing studies have sought to mitigate the time required to annotate while simultaneously not compromising performance. Bearman et al. introduce the concept of image-level, squiggle-level, and point-level supervised segmentation, along with the average annotation time and evaluation performance for each type [8]. The study performed three-types of weakly-supervised annotation schemes on the Pascal-VOC dataset, and compared their annotation times and performance to full segmentation masks. Point-level supervision requires one or more points annotated per class object, as opposed to full pixel-accurate painting, taking an average of 22.1 seconds per image. Squiggle-level supervision, similarly, requires one or more “squiggles”, or continuous series of points per image, averaging 34.9 seconds per image. In comparison, full segmentation mask painting took an average of 239.7 seconds per image - nearly 7 times slower than squiggle-level annotation and over 10 times slower than point-level annotation.

### C. Point-Supervised Segmentation

One method of weakly-supervised segmentation only requires the annotation of only a small, variable number of

points to be annotated, rather than painted over entirely. Point-supervised segmentation, namely, has been supported by recent research to be a viable solution to the costly process of segmentation annotation. In addition to the study performed by Bearman et al. [8], Cheng et al. outline a simple, yet effective point annotation scheme, where only 10 points are selected and classified within a bounding box of an object [7]. Trained on Mask R-CNN and evaluated only on annotated points, this annotation scheme achieved up to 98% of its fully-supervised performance, despite being nearly 5 times faster to annotate point-wise. Cheng et al. further show that applying the paradigm of transfer learning by pretraining on existing large-scale segmentation data prior to training on point annotations is equally effective - both in the case of full masks of the larger dataset being available, as well as when only point annotations of said dataset are available [7].

## III. METHOD

### A. Datasets

We use two primary datasets, depicted in Table I, to explore weakly-supervised learning and its application to ship segmentation:

Dataset	Domain	# Images	Resolution	Label Scheme
Airbus	Visible	200,000	780x780	Full mask
NAWCAD	Infrared	7,000	640x480	Unlabeled

TABLE I: Details of the two datasets used during training.

The Airbus dataset [16], consists of clear, high-resolution RGB images taken from a flat aerial perspective, shown in Figure 2. The NAWCAD (Naval Air Warfare Center Aircraft Division) dataset, however, includes comparatively-lower resolution infrared images, with only a fraction of the volume of the Airbus set. The NAWCAD dataset contains 7055 unlabeled infrared images taken from an unmanned aerial vehicle, in both white-hot and black-hot formats. In contrast to the Airbus images, NAWCAD images were captured with varying angles and environmental conditions. All NAWCAD images were collected from the bay area of the Patuxent River in Maryland. A sample of the dataset is displayed in Figure 3. Given the generally-limited availability of infrared images, along with the additional limitations of the NAWCAD images, we aimed to utilize the external Airbus dataset to supplement the weakly-supervised learning process, via transfer learning. In order to determine a baseline potential for weakly-supervised segmentation, we train with a random sample of mask pixels from the fully-segmented Airbus set. Each pixel is labeled as either boat or background. The dataset contains some overlap between nearby boats, landmasses, or other objects, but the majority of objects are isolated in open water. We randomly mask  $n\%$  of all pixel labels, at both the both at  $n=95\%$  and  $n=90\%$  levels. The generated masks were then sent through the data pipeline as the ground truth for the model. A comparison of full labeled data (no mask) to a 95% mask can be seen in Figure 4.



Fig. 2: Example images from the Airbus dataset [17]. These satellite images are clean of any post-processing markings, ships are visually identifiable, and the interference from structures or landmasses is low.

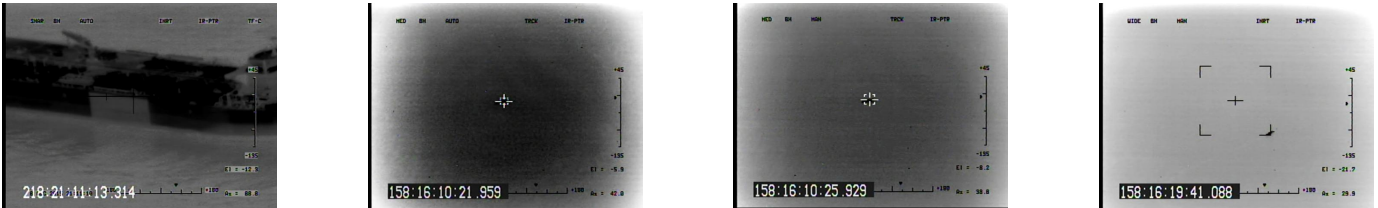


Fig. 3: Example images from the NAWCAD dataset. These images contain post processing marks such as scales, crosshairs, and time stamps imposed onto the image.

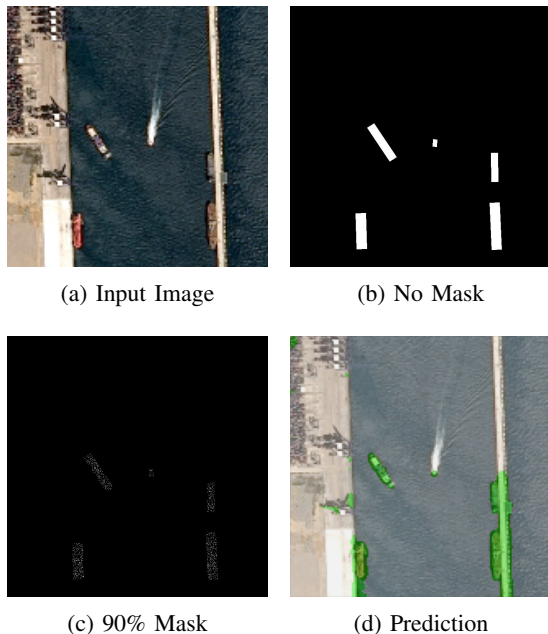


Fig. 4: We show the different configurations of training labels that were used for testing the hypothesis of using subsampled data to train a segmentation network.

### B. Data Preparation

Inspired by the results using weak supervision on the Airbus dataset, we explore two annotation schemes for labeling the NAWCAD IR dataset, shown in Figure 5. The first method - *point* annotation - involves selecting 5 points for each class (namely, the ship and background class) to allow for an even sample distribution across all classes. The second method - *squiggle* annotation - involves drawing squiggle lines on

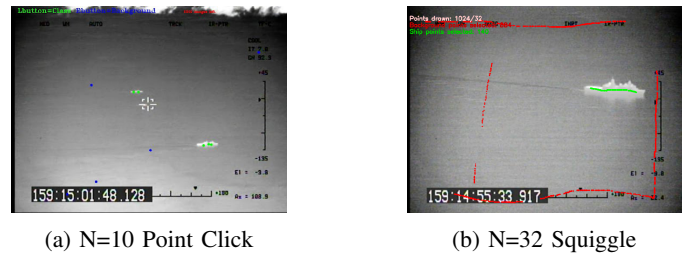


Fig. 5: Example displaying the different annotation schemes used to create labels. (a) Shows the point annotation method where 10 points are sampled with an even distribution between ship and background. (b) Shows the use of drawing lines/squiggles on the image, from which we extract 32 random points weighted by the proportion of points drawn per class.

each class, from which a weighted random sample of 32 points are selected. Squiggle annotation allows for a larger, more scaled sample of points to be considered while training, while still taking around the same amount of time as point annotation. We annotated 1200 infrared images using the point-supervised and squiggle-supervised annotation schemes. Once all images were annotated using the respective methods, the new dataset was randomly shuffled and then split into 90% training / 10% validation sets, due to limited amount of trainable images. Prior to training, the dataset is augmented via standard segmentation transformations, including random shuffling, rotation, scaling, and cropping.

### C. Loss Function

Pixel-Wise Cross-Entropy (PWCE) was used to train both annotation schemes. PWCE is an implementation inspired by



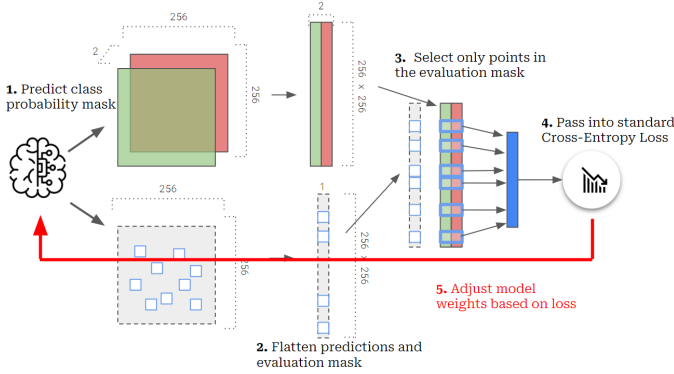


Fig. 6: This diagram visually illustrates how the labels and evaluation mask are applied to the loss function during training.

the original study introducing point-wise supervision [7], with our method of point sampling in mind.

$$L_{PWCE}(Y, \hat{Y}, m) = - \sum_{i=1}^n [(Y_i m_i) * \log(\hat{Y}_i m_i)] \quad (1)$$

A diagram of the process is shown in figure 6.

During the generation of the dataset, the loader creates three different images; the original image, the ground truth annotated points, and an evaluation mask denoting which points in the ground truth label to evaluate on (represented as a sparse boolean array). This way, points not to be considered in evaluation are zeroed out by the mask, and not factored into the loss function.

#### D. Transfer Learning

Due to the limitations of the NAWCAD dataset, as mentioned in III-A, we explore the effectiveness of transfer learning in combination with augmentation techniques. This would ideally allow the network to better generalize previous strongly-learned features of interest to our weakly-supervised task, along with reducing total training time. We applied transfer learning for both point-supervised and squiggle-supervised annotation schemes. The model was first pretrained on the full Airbus dataset, with grayscaling and random inversion augmentations applied to account for the domain change to both formats of thermal images. The goal of doing this was to assist the model with identifying boat shapes and edges in contrast with the background scenery.

## IV. RESULTS

This section demonstrates the difference in performance when utilizing 10 evenly distributed samples versus 32 randomly distributed samples. For our analysis we created a subset of fully segmented images that were not used during training for inference. The predictions are scored against the inference labels by measuring the precision, recall and Jaccard index score. The Jaccard score gives us quantitative metric of accuracy that measures the ratio of correct pixel-wise classifications to the total number of classifications. It is defined as:

$$J(A, B) = \frac{|A \cup B|}{|A| + |B| - |A \cap B|}$$

#### A. 32-point Subsample Results

The success cases from the squiggle annotations of the IR dataset are displayed in the last row of Table II. An outline of the training performance is shown in Tables III and IV. We observe that even with a massive reduction in trainable labels, the performance of the model is still admirable. However, as displayed in the last two columns of Table II, due to the low amount of overall training image variety, eliminating false positives completely and achieving full segmentation from the model still pose a problem, especially in heavy atmospheric conditions.

#### B. 10-point Subsample Results

The analysis for this training scheme is depicted in Tables III and IV. These tables depict that with further reduction of the trainable labels, the model still performs relatively similar to the 32-point training regime. The second row of Table II displays a visual representation of predictions generated during inference. The first three columns show the success cases which our model performed optimally; these images show that with little to no environmental noise, a model trained on only point-annotated labels performs well. However, as seen in the last two columns, the model begins to falter and over segment in the presence of boat wake trails and cloud coverage. In addition, we observe that segmentation tends to falter on large ships that extend beyond the frame of the image.

## V. CONCLUSION

In this work, we illustrate that a weakly-supervised annotation scheme can be effectively used to perform thermal image segmentation in high-noise, maritime environments, from only several hundred training samples. Despite taking substantially less time for annotation compared to full segmentations, point-supervised segmentation can be used to successfully and robustly detect and segment both large and small ships. We also investigate the effect of transfer learning from full segmentations in the visible domain (RGB) on weakly-supervised segmentation, finding that pre-training on similar ship image data marginally improves performance after training for the same number of epochs. While we still observed certain phenomena (such as clouds or boat trails) affecting detection performance on occasion, this was not the case the majority of the time. As a part of future work, annotating and training on more images containing prevalent cloud coverage and boat trails would likely improve detection accuracy.<sup>1</sup>

#### ACKNOWLEDGEMENTS

This work was supported by the University of Maryland Applied Research Lab for Intelligence and Security (ARLIS) and the Naval Air Warfare Center Aircraft Division (NAWCAD), as a part of the Research for Intelligence and Security Challenges (RISC) internship program. Metzler was supported in part by the AFOSR Young Investigator Program.

<sup>1</sup>Link to code and data: [Github](#)

## REFERENCES

- [1] *How long is the U.S. shoreline?* July 2010. URL: <https://oceanservice.noaa.gov/facts/shorelength.html#:~:text=NOAA's%20official%20value%20for%20the,U.S.%20shoreline%20is%5C%2095%5C%2C471%5C%20miles>.
- [2] Department of Defense Inspector General Office. *Evaluation of Contract Monitoring and Management for Project Maven*. DOD Report No. DODIG-2022-049. 4800 Mark Center Drive Alexandria, Virginia 223500-1500, 2022. URL: <https://media.defense.gov/2022/Jan/10/2002919460/-1/-1/1/DODIG-2022-049-REDACTED.PDF>.
- [3] Maxence Chaverot et al. “Object Detection on Thermal Images: Performance of YOLOv4 Trained on Small Datasets”. In: Jan. 2021, pp. 207–212. DOI: [10.14428/esann/2021.ES2021-130](https://doi.org/10.14428/esann/2021.ES2021-130).
- [4] Elizabeth Bondi et al. “BIRDSAI: A Dataset for Detection and Tracking in Aerial Thermal Infrared Videos”. In: *2020 IEEE Winter Conference on Applications of Computer Vision (WACV)*. 2020, pp. 1736–1745. DOI: [10.1109/WACV45572.2020.9093284](https://doi.org/10.1109/WACV45572.2020.9093284).
- [5] Yung-Yao Chen, Wei-Sheng Chen, and Hui-Sheng Ni. “Image segmentation in thermal images”. In: *2016 IEEE International Conference on Industrial Technology (ICIT)*. 2016, pp. 1507–1512. DOI: [10.1109/ICIT.2016.7474983](https://doi.org/10.1109/ICIT.2016.7474983).
- [6] Zülfiye Küttük and Görkem Algan. *Semantic Segmentation for Thermal Images: A Comparative Survey*. May 2022. DOI: [10.48550/arXiv.2205.13278](https://doi.org/10.48550/arXiv.2205.13278).
- [7] Bowen Cheng, Omkar Parkhi, and Alexander Kirillov. “Pointly-Supervised Instance Segmentation”. In: *CoRR* abs/2104.06404 (2021). arXiv: [2104.06404](https://arxiv.org/abs/2104.06404). URL: <https://arxiv.org/abs/2104.06404>.
- [8] Amy Bearman et al. “What’s the Point: Semantic Segmentation with Point Supervision”. In: *Computer Vision – ECCV 2016*. Ed. by Bastian Leibe et al. Cham: Springer International Publishing, 2016, pp. 549–565. ISBN: 978-3-319-46478-7.
- [9] Zihao Dong et al. “Scale-Recursive Network with point supervision for crowd scene analysis”. In: *Neurocomputing* 384 (2020), pp. 314–324. ISSN: 0925-2312. DOI: <https://doi.org/10.1016/j.neucom.2019.12.070>. URL: <https://www.sciencedirect.com/science/article/pii/S0925231219317795>.
- [10] Akshay L. Chandra et al. “Active learning with point supervision for cost-effective panicle detection in cereal crops”. In: *Plant Methods* 16.1 (2020). DOI: [10.1186/s13007-020-00575-8](https://doi.org/10.1186/s13007-020-00575-8).
- [11] Olaf Ronneberger, Philipp Fischer, and Thomas Brox. “U-Net: Convolutional Networks for Biomedical Image Segmentation”. In: *CoRR* abs/1505.04597 (2015). arXiv: [1505.04597](https://arxiv.org/abs/1505.04597). URL: <http://arxiv.org/abs/1505.04597>.
- [12] Vijay Badrinarayanan, Alex Kendall, and Roberto Cipolla. *SegNet: A Deep Convolutional Encoder-Decoder Architecture for Image Segmentation*. 2015. DOI: [10.48550/ARXIV.1511.00561](https://doi.org/10.48550/ARXIV.1511.00561). URL: <https://arxiv.org/abs/1511.00561>.
- [13] Kaiming He et al. *Mask R-CNN*. 2017. DOI: [10.48550/ARXIV.1703.06870](https://doi.org/10.48550/ARXIV.1703.06870). URL: <https://arxiv.org/abs/1703.06870>.
- [14] Hao Zhang et al. “Infrared Image Segmentation for Photovoltaic Panels Based on Res-UNet”. In: Oct. 2019, pp. 611–622. ISBN: 978-3-030-31653-2. DOI: [10.1007/978-3-030-31654-9\\_52](https://doi.org/10.1007/978-3-030-31654-9_52).
- [15] Tsung-Yi Lin et al. “Microsoft COCO: Common Objects in Context”. In: *CoRR* abs/1405.0312 (2014). arXiv: [1405.0312](https://arxiv.org/abs/1405.0312). URL: <http://arxiv.org/abs/1405.0312>.
- [16] *Airbus Ship Detection Challenge*. July 2018. URL: <https://www.kaggle.com/competitions/airbus-ship-detection/data>.
- [17] Zhengning Zhang et al. “ShipRSImageNet: A Large-scale Fine-Grained Dataset for Ship Detection in High-Resolution Optical Remote Sensing Images”. In: *IEEE Journal of Selected Topics in Applied Earth Observations and Remote Sensing* PP (Aug. 2021), pp. 1–1. DOI: [10.1109/JSTARS.2021.3104230](https://doi.org/10.1109/JSTARS.2021.3104230).
- [18] Simon Jégou et al. “The One Hundred Layers Tiramisu: Fully Convolutional DenseNets for Semantic Segmentation”. In: *CoRR* abs/1611.09326 (2016). arXiv: [1611.09326](https://arxiv.org/abs/1611.09326). URL: <http://arxiv.org/abs/1611.09326>.
- [19] Jonathan Sauder and Bjarne Sievers. “Self-Supervised Deep Learning on Point Clouds by Reconstructing Space”. In: *Advances in Neural Information Processing Systems*. Ed. by H. Wallach et al. Vol. 32. Curran Associates, Inc., 2019. URL: <https://proceedings.neurips.cc/paper/2019/file/993edc98ca87f7e08494eec37fa836f7-Paper.pdf>.
- [20] Ratner Alex and Varma Paroma. *Weak supervision: A new programming paradigm for Machine Learning*. <http://ai.stanford.edu/blog/weak-supervision/>. Mar. 2019.
- [21] Jonathan Sauder and Bjarne Sievers. “Context Prediction for Unsupervised Deep Learning on Point Clouds”. In: *CoRR* abs/1901.08396 (2019). arXiv: [1901.08396](https://arxiv.org/abs/1901.08396). URL: <http://arxiv.org/abs/1901.08396>.
- [22] Utsav B. Gewali and Sildomar T. Monteiro. “A Tutorial on Modeling and Inference in Undirected Graphical Models for Hyperspectral Image Analysis”. In: *CoRR* abs/1801.08268 (2018). arXiv: [1801.08268](https://arxiv.org/abs/1801.08268). URL: <http://arxiv.org/abs/1801.08268>.
- [23] Bigironsphere. *Loss function library - keras & pytorch*. July 2021. URL: <https://www.kaggle.com/code/bigironsphere/loss-function-library-keras-pytorch/notebook>.
- [24] Aäron van den Oord, Yazhe Li, and Oriol Vinyals. “Representation Learning with Contrastive Predictive Coding”. In: *CoRR* abs/1807.03748 (2018). arXiv: [1807.03748](https://arxiv.org/abs/1807.03748). URL: <http://arxiv.org/abs/1807.03748>.
- [25] Maxime Oquab et al. “Is Object Localization for Free? - Weakly-Supervised Learning With Convolutional Neural Networks”. In: *Proceedings of the IEEE Conference on Computer Vision and Pattern Recognition (CVPR)*. June 2015.

- [26] Yuewei Yang, Kevin J. Liang, and Lawrence Carin. “Object Detection as a Positive-Unlabeled Problem”. In: *CoRR* abs/2002.04672 (2020). arXiv: 2002.04672. URL: <https://arxiv.org/abs/2002.04672>.
- [27] Aishwarya Kamath et al. “MDETR - Modulated Detection for End-to-End Multi-Modal Understanding”. In: *CoRR* abs/2104.12763 (2021). arXiv: 2104.12763. URL: <https://arxiv.org/abs/2104.12763>.
- [28] Pravendra Singh et al. “Multi-layer Pruning Framework for Compressing Single Shot MultiBox Detector”. In: *CoRR* abs/1811.08342 (2018). arXiv: 1811.08342. URL: <http://arxiv.org/abs/1811.08342>.
- [29] Lisang Liu et al. “Ship infrared image edge detection based on an improved adaptive Canny algorithm”. In: *International Journal of Distributed Sensor Networks* 14.3 (2018), p. 1550147718764639. DOI: 10.1177/1550147718764639. eprint: <https://doi.org/10.1177/1550147718764639>. URL: <https://doi.org/10.1177/1550147718764639>.
- [30] Jun-Yan Zhu et al. “Unpaired Image-to-Image Translation using Cycle-Consistent Adversarial Networks”. In: *CoRR* abs/1703.10593 (2017). arXiv: 1703.10593. URL: <http://arxiv.org/abs/1703.10593>.
- [31] Phillip Isola et al. “Image-to-Image Translation with Conditional Adversarial Networks”. In: *CoRR* abs/1611.07004 (2016). arXiv: 1611.07004. URL: <http://arxiv.org/abs/1611.07004>.
- [32] Olcay Kursun and Ethem Alpaydin. “Canonical Correlation Analysis for Multiview Semisupervised Feature Extraction”. In: *Artificial Intelligence and Soft Computing*. Ed. by Leszek Rutkowski et al. Berlin, Heidelberg: Springer Berlin Heidelberg, 2010, pp. 430–436. ISBN: 978-3-642-13208-7.
- [33] Matthias Limmer and Hendrik P. A. Lensch. “Infrared Colorization Using Deep Convolutional Neural Networks”. In: *CoRR* abs/1604.02245 (2016). arXiv: 1604.02245. URL: <http://arxiv.org/abs/1604.02245>.
- [34] Mingsong Dou et al. “Converting Thermal Infrared Face Images into Normal Gray-Level Images”. In: Nov. 2007, pp. 722–732. ISBN: 978-3-540-76389-5. DOI: 10.1007/978-3-540-76390-1\_71.
- [35] *Ships Dataset*. <https://makeml.app/datasets/ships>.
- [36] Muhammad Waseem Ashraf, Waqas Sultani, and Mubarak Shah. “Dogfight: Detecting Drones From Drones Videos”. In: *Proceedings of the IEEE/CVF Conference on Computer Vision and Pattern Recognition (CVPR)*. June 2021, pp. 7067–7076.
- [37] Robotic Automation Expert. “Introducing transfer learning as your next engine to drive future innovations”. <https://medium.datadriveninvestor.com/introducing-transfer-learning-as-your-next-engine-to-drive-future-innovations-5e81a15bb567>. Feb. 2020.
- [38] Doaa Shoieb, Sherin Youssef, and Walid Aly. “Computer-Aided Model for Skin Diagnosis Using Deep Learning”. In: *Journal of Image and Graphics* 4 (Dec. 2016), pp. 116–121. DOI: 10.18178/joig.4.2.122-129.
- [39] Marina Ivašić-Kos, Mate Krišto, and Miran Pobar. “Human Detection in Thermal Imaging Using YOLO”. In: Apr. 2019, pp. 20–24. DOI: 10.1145/3323933.3324076.
- [40] Zhi-Hua Zhou. “A Brief Introduction to Weakly Supervised Learning”. In: *National Science Review* 5 (Aug. 2017). DOI: 10.1093/nsr/nwx106.

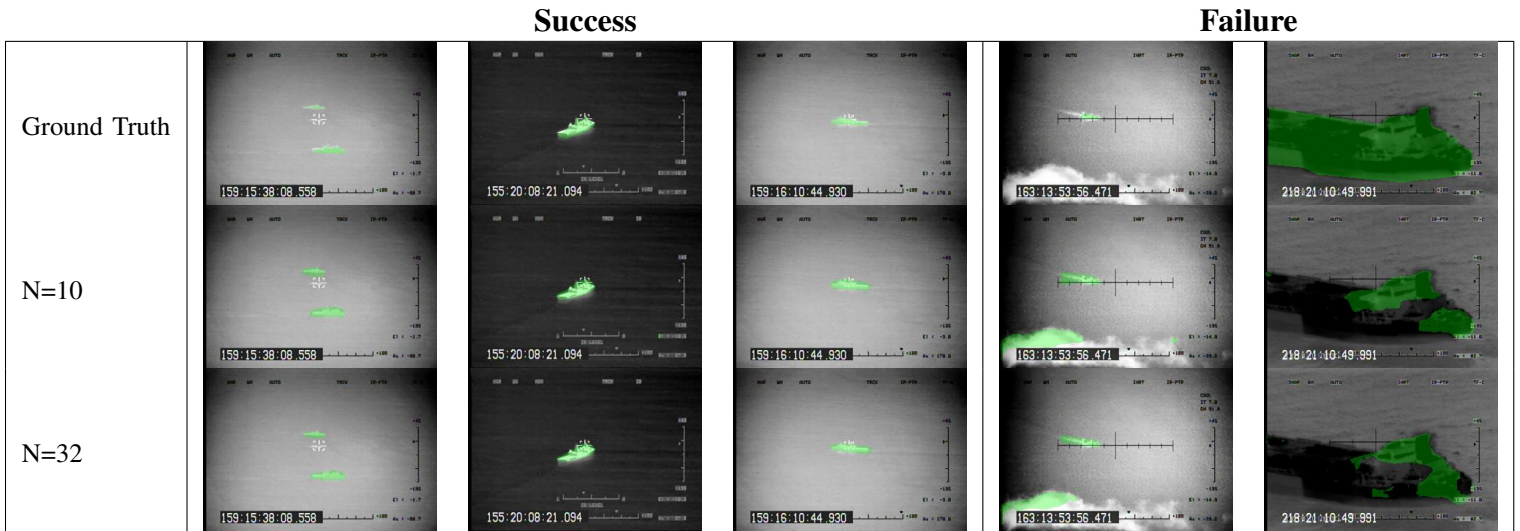


TABLE II: Success and failure cases of segmentation mask predictions, using the two different annotation schemes.

Supervision	Augmentations	Precision	Recall	Jaccard Score
Squiggle (n=32)	None	.925	.948	.612
Squiggle (n=32)	Grayscale and Inversion	.979	.978	.756
Point (n=10)	Grayscale and Inversion	.976	.976	.692

TABLE III: Calculated Precision, Recall and Jaccard scores of the inference image mask predictions made by a network pre-trained on the Airbus dataset, scored against a limited set of test images with full segmentation maps.

Supervision	Augmentations	Precision	Recall	Jaccard Score
Squiggle (n=32)	None	.891	.922	.601
Squiggle (n=32)	Grayscale and Inversion	.972	.973	.726
Point (n=10)	Grayscale and Inversion	.961	.962	.687

TABLE IV: Calculated Precision, Recall and Jaccard scores of the inference image mask predictions made by a non-pretrained network, scored against a limited set of test images with full segmentation maps.